An *ab initio* study of the reaction of atomic hydrogen with sulfur dioxide

Derk Binns and Paul Marshall
Department of Chemistry, University of North Texas, PO Box 5068, Denton, Texas 76203

(Received 23 May 1991; accepted 25 June 1991)

The potential energy surface for $H(1\,^2S) + SO_2$ has been investigated computationally in order to study the catalytic removal of atomic hydrogen in flames by sulfur dioxide. HF/3–21G(*) and MP2/3–21G(*) levels of theory were employed to locate stationary points, which were then characterized by calculation of the vibrational frequencies. Some geometries were also optimized with the 6–31G* basis set. Two adducts HOSO and HSO_2, with H bonded to O or S, respectively, were studied. Energies were estimated at the optimized geometries using spin-projected MP4/6–31G* calculations, which show that planar *cis* HOSO is more stable than C_s HSO_2. An H–OSO bond energy of 109 kJ mol^{-1} is predicted. By contrast HSO_2 is predicted to be 25 kJ mol^{-1} endothermic with respect to $H + SO_2$, and is insufficiently stable to be significant in combustion chemistry. Transition states were located and the information used to derive the kinetics of $H + SO_2 + Ar \rightleftarrows HOSO + Ar$ from 298 to 2000 K. An unusually large energy barrier to recombination, of about 95 kJ mol^{-1} relative to $H + SO_2$, is proposed. The results are compared with available kinetic measurements. Other potential decomposition channels for HOSO, to SO + OH and isomerization to HSO_2, were also analyzed.

I. INTRODUCTION

Addition of sulfur dioxide to flames reduces the concentration of atomic hydrogen, a phenomenon which is attributed to catalysis of H-atom recombination via formation of an adduct between H and SO_2,[1–6]

$$H + SO_2(+M) \rightarrow SO_2{\cdot}H(+M), \quad (1)$$

$$SO_2{\cdot}H + H \rightarrow SO_2 + H_2. \quad (2)$$

Provided reaction (1) maintains an equilibrium $[SO_2{\cdot}H]$, the overall loss of H atoms will be second order in [H]. Experimental data from SO_2-seeded flames thus yields the product K_1k_2, where K_1 is the equilibrium constant for reaction (1) and k_2 is the rate constant for reaction (2).[3,4,6] Kallend estimated that the SO_2–H bond energy D_0 is at least 200 kJ mol^{-1}, and probably between 210 and 250 kJ mol^{-1}, based on observations of emission from $Na(3\,^2P)$ believed to be excited by reaction (1) with M = Na.[2] Later workers employed $D_0 = 264$ kJ mol^{-1}.[3,4]

A potential interference in combustion studies of the elementary reaction (1) is the complex network of reactions which interconverts the many reactive intermediates present in a flame. One experiment designed to isolate reaction (1) from other processes set an upper limit to k_1 of $< 1.5\times10^{-33}$ cm^6 molecule^{-2} s^{-1} at room temperature.[7] This upper limit, coupled with flame measurements, implies an unusual positive activation energy for this recombination reaction of at least 12 kJ mol^{-1} and the presence of a significant barrier to adduct formation.[8] Preliminary isolated reaction studies carried out in this laboratory confirm the upper limit to k_1 of $< 1.5\times10^{-33}$ cm^6 molecule^{-2} s^{-1} at 298 K, and extend this same limiting value up to 500 K.[9] These experiments[7,9] disagree with the results of Gordon *et al.*,[10] who estimated a room temperature rate constant of 6×10^{-33} cm^6 molecule^{-2} s^{-1}. The $SO_2{\cdot}H$ radical is significant in contexts aside from combustion chemistry. It has been proposed as a reactive intermediate in the high-temperature reduction of SO_2 by H_2,[11] and may also be relevant to the atmospheric chemistry of sulfur: Howard and coworkers proposed $SO_2{\cdot}H$ as the product of the reaction of HSO with NO_2 at room temperature, and found it reacted readily with O_2 to form HO_2.[12]

The geometry of the $SO_2{\cdot}H$ adduct is uncertain. Two possible structures have the H atom bonded either to the S atom, represented here as HSO_2, or bonded to an O atom, represented here as HOSO. The only experimental geometry information to date is from a study by McDowell *et al.*,[13] who photolyzed a mixture of HI and SO_2 in a frozen Kr matrix. After repeated annealing, the electron spin resonance (ESR) spectrum of a species identified as C_s HSO_2 was obtained. This HSO_2 adduct has been the subject of two *ab initio* molecular orbital studies, by Hinchliffe[14] and by Boyd *et al.*[15] The latter work yielded a H–SO_2 bond energy of 142 kJ mol^{-1}, a value which is presently recommended for use in modeling atmospheric chemistry[16] although this bond energy is 60 to 120 kJ mol^{-1} lower than those employed in the combustion studies noted above. Boyd *et al.* also investigated the possible HOSO adduct and found it to be the more stable structure.

The aim of the present work is to investigate the HSO_2 and HOSO adducts by means of *ab initio* computational methods, in order to obtain information about the likely thermochemistry of reaction (1). For the first time vibrational frequencies are calculated, which should aid attempts to identify matrix-isolated species by IR spectroscopy, and electron correlation is taken into account. The first theoretical study of transition states in the $H + SO_2$ potential energy surface (PES) is carried out to permit a kinetic analysis of reaction (1) and possible isomerization between the two $SO_2{\cdot}H$ structures.

 0021-9606/91/194940-08$03.00

II. METHODOLOGY

Standard computational methods, described in detail elsewhere,[17] were applied by means of the GAUSSIAN 88 program[18] implemented on a VAX 6310 computer and GAUSSIAN 90[19] on a Cray Y-MP/832. Stationary points on the PES for $H + SO_2$ were initially located using the 3–21G(*) atomic basis set[20] at the Hartree–Fock (HF) level. This basis set includes *d*-type polarization functions on the S atom. Spin-restricted HF was employed for closed-shell SO_2, and unrestricted HF for the open-shell species. We denote these results as HF/3–21G(*). Harmonic vibrational frequencies ν_e were calculated at each stationary point to characterize it as a true minimum or a transition state (TS) with a single imaginary frequency. These ν_e are scaled by a standard factor of 0.9 to approximate ν_0.[17] In some cases the geometry was also optimized with the larger 6–31G* basis set,[21] which includes *d*-type polarization functions on S and O, to test for any dependence of bond angles and lengths on the size of the atomic basis set.

The geometries of the stationary points were then reoptimized while making a correction for electron correlation by means of Møller–Plesset (MP) second-order perturbation theory for all electrons. Vibrational frequencies were also calculated at this MP2/3–21G(*) level. We verified the stability of the HF wave function at each stationary point.[22] Finally, we employed the 6–31G* basis set to calculate the energy at each MP2/3–21G(*) geometry using MP4 theory (excluding core electrons). Spin-contamination effects on the energies were eliminated by Schlegel's projection method,[23] and the final results are denoted as PMP4/6–31G*//MP2/3–21G(*) energies.

III. RESULTS AND DISCUSSION

The *ab initio* geometries, vibrational frequencies, and energies are summarized in Tables I and II and Fig. 1. Three stable minima, corresponding to $H + SO_2$, HOSO, and HSO_2, and transition states (TS) between them are discussed below. Figure 2 is a diagram of the vibrationally adia-

TABLE I. *Ab initio* geometries and frequencies for stationary points on the $H + SO_2$ PES.

Species	Calculation	Geometry[a] and frequencies[b]
$C_{2v}SO_2$	HF/3–21G(*)	$\theta = 118.7$, $r(SO) = 1.419$ $\nu = 541, 1208, 1417$
	MP2/3–21G(*)	$\theta = 120.0$, $r(SO) = 1.485$ $\nu = 493, 1034, 1291$
C_sHSO_2	HF/3–21G(*)	$\theta = 122.5$, $\psi = 106.8$, $r(SO) = 1.447$, $r(SH) = 1.340$ $\nu = 461, 839, 916, 1018, 1196, 2426$
	MP2/3–21G(*)	$\theta = 125.1$, $\psi = 106.4$, $r(SO) = 1.480$, $r(SH) = 1.379$ $\nu = 453, 857, 1131, 1249, 2309, 3401$
	HF/6–31G*	$\theta = 123.6$, $\psi = 106.6$, $r(SO) = 1.439$, $r(SH) = 1.340$
$HSO_2 \rightarrow H + SO_2$ TS	MP2/3–21G(*)	$\theta = 121.2$, $\psi = 105.1$, $r(SO) = 1.469$, $r(SH) = 1.839$ $\nu = \cdots$
cis HOSO	HF/3–21(G*)	$\theta = 107.1$, $\phi = 114.8$, $r(SO_1) = 1.484$, $r(SO_2) = 1.629$, $r(HO_2) = 0.972$ $\nu = 243i, 370, 771, 977, 1061, 3443$
	MP2/3–21G(*)	$\theta = 111.4$, $\phi = 111.0$, $r(SO_1) = 1.480$, $r(SO_2) = 1.662$, $r(HO_2) = 1.001$ $\nu = 107, 355, 784, 1102, 1483, 3458$
	HF/6–31G*	$\theta = 107.4$, $\phi = 109.9$, $r(SO_1) = 1.461$, $r(SO_2) = 1.625$, $r(HO_2) = 0.955$
Staggered HOSO	HF/3–21G(*)	$\theta = 107.5$, $\phi = 115.2$, $\delta = 74.7$, $r(SO_1) = 1.510$, $r(SO_2) = 1.624$, $r(HO_2) = 0.970$ $\nu = 337, 403, 754, 854, 1102, 3438$
	HF/6–31G*	$\theta = 108.2$, $\phi = 111.5$, $\delta = 59.5$, $r(SO_1) = 1.468$, $r(SO_2) = 1.623$, $r(HO_2) = 0.953$
trans HOSO	HF/3–21G(*)	$\theta = 104.3$, $\phi = 114.0$, $r(SO_1) = 1.486$, $r(SO_2) = 1.637$, $r(HO_2) = 0.970$ $\nu = 370i, 384, 750, 927, 1014, 3457$
	MP2/3–21G(*)	$\theta = 108.6$, $\phi = 110.7$, $r(SO_1) = 1.469$, $r(SO_2) = 1.667$, $r(HO_2) = 0.996$ $\nu = 283i, 399, 779, 1055, 1500, 3489$
	HF/6–31G*	$\theta = 105.3$ $\phi = 110.1$, $r(SO_1) = 1.456$, $r(SO_2) = 1.632$, $r(HO_2) = 0.952$
HOSO → H + SO_2 TS	HF/3–21G(*)	$\theta = 110.8$, $\phi = 116.1$, $\delta = 87.2$, $r(SO_1) = 1.499$, $r(SO_2) = 1.539$, $r(HO_2) = 1.785$ $\nu = 713i, 248, 411, 446, 675, 866$
	MP2/3–21G(*)	$\theta = 120.5$, $\phi = 124.9$, $\delta = 81.8$, $r(SO_1) = 1.441$, $r(SO_2) = 1.467$, $r(HO_2) = 1.550$ $\nu = 2241i, 324, 528, 612, 1159, 1619$
	HF/6–31G*	$\theta = 112.8$, $\phi = 116.5$, $\delta = 84.7$, $r(SO_1) = 1.457$, $r(SO_2) = 1.514$, $r(HO_2) = 1.664$
HOSO → HSO_2 TS	HF/3–21G(*)	$\theta = 113.8$, $\phi = 60.7$, $\delta = 105.3$, $r(SO_1) = 1.448$, $r(SO_2) = 1.624$, $r(HO_2) = 1.367$ $\nu = 2127i, 411, 699, 760, 1189, 1603$
	MP2/3–21G(*)	$\theta = 118.1$, $\phi = 57.4$, $\delta = 106.6$, $r(SO_1) = 1.481$, $r(SO_2) = 1.629$, $r(HO_2) = 1.392$ $\nu = 2114i, 423, 719, 842, 1242, 2359$
	HF/6–31G*	$\theta = 114.0$, $\phi = 60.6$, $\delta = 104.9$, $r(SO_1) = 1.438$, $r(SO_2) = 1.598$, $r(HO_2) = 1.351$

[a] See Fig. 1 for definitions of the coordinates. Angles are in degrees and distances are in Å.
[b] Frequencies are in cm^{-1} and were calculated only with the 3–21G(*) basis set. HF results are scaled by a factor of 0.9, while MP2 results are unscaled.

TABLE II. *Ab initio* energies for stationary points on the H + SO_2 PES.

Species	Calculation	Energy, au	$\langle S^2 \rangle$	ΔH_0, kJ mol^{-1} [a]
H	HF/3–21G(*)	−0.4962	0.75	
	HF/6–31G*	−0.4982	0.75	
OH	HF/3–21G(*)	−74.9702	0.75	
	MP2/3–21G(*)	−75.0572	0.75	
	PMP4/6–31G*//MP2/3–21G(*)	−75.5367	0.76	
SO	HF/3–21G(*)	−470.0747	2.03	
	PMP4/6–31G*//HF/3–21G(*)	−472.6361	2.04	
$C_{2v}SO_2$	HF/3–21G(*)	−544.5037	0	
	MP2/3–21G(*)	−544.9203	0	
	PMP4/6–31G*//MP2/3–21G(*)	−547.7111	0	
C_sHSO_2	HF/3–21G(*)	−545.0213	0.78	
	MP2/3–21G*	−545.4125	0.78	
	PMP4/6–31G*//MP2/3–21G(*)	−548.2149	0.78	+25
H + SO_2→HSO_2TS	MP2/3–21G(*)	−545.3939	0.89	
cis HOSO	HF/3–21G(*)	−545.0873	0.77	
	MP2/3–21G(*)	−545.4553	0.77	
	PMP4/6–31G*//MP2/3–21G(*)	−548.2611	0.77	−109
Staggered HOSO	HF/3–21G(*)	−545.0903	0.76	
trans HOSO	HF/3–21G(*)	−545.0785	0.76	
	MP2/3–21G(*)	−545.4444	0.77	
	PMP4/6–31G*//MP2/3–21G(*)	−548.2537	0.77	−90
HOSO→H + SO_2TS	HF/3–21G(*)	−544.9986	1.44	
	MP2/3–21G(*)	−545.3616	1.14	
	PMP4/6–31G*//MP2/3–21G(*)	−548.1763	1.10	+95
HOSO→HSO_2TS	HF/3–21G(*)	−544.9725	0.89	
	MP2/3–21G(*)	−545.3579	0.85	
	PMP4/6–31G*//MP2/3–21G(*)	−548.1694	0.84	+121

[a] Enthalpy at 0 K relative to H + SO_2, using PMP4/6–31G*//MP2/3–21G(*) energies combined with zero-point energies calculated at the MP2/3–21G(*) level.

batic ground-state PES which corresponds to the enthalpy surface at 0 K, i.e., the electronic energy plus zero-point vibrational energy (ZPE). Spin-conservation was assumed, i.e., all stationary points are doublet states. A channel leading to OH + SO has also been analyzed.

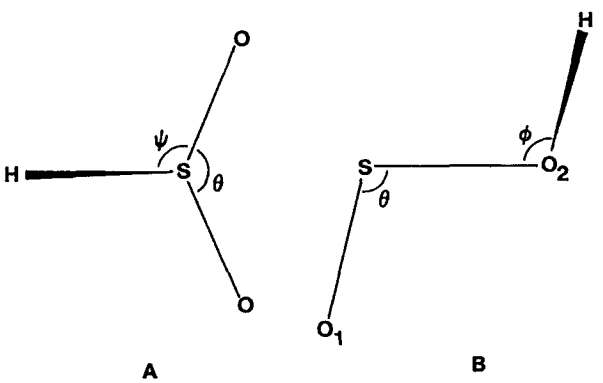

FIG. 1. Sketch of molecular structures showing definitions of bond angles for (A) HSO_2 and (B) HOSO. The dihedral angle O_1SO_2H is δ.

A. SO_2, OH, and SO

It is important to estimate the likely accuracy of these calculations, which we do by comparison with data for experimentally known species. There is reasonable accord between experimental and theoretical geometries for SO_2. The calculated bond lengths bracket the experimental value of 1.432 Å (1 Å = 10^{-10} m):[24] The HF/3–21G(*) distances are about 0.01 Å too small while the higher level MP2/3–21G(*) calculations overestimate r(SO) by about 0.05 Å. Similarly, the calculated vibrational frequencies bracket the experimental values of 518, 1151, and 1362 cm^{-1}.[24] The scaled HF/3–21G(*) estimates are 7% too high whereas the (unscaled) MP2/3–21G(*) estimates are 7% too low. Based on these comparisons, we assign approximate error limits of ± 0.05 Å for calculated bond lengths and ± 10% for calculated vibrational frequencies.

The HF/3–21G(*) and MP2/3–21G(*) bond lengths for OH are 0.985 and 1.006 Å, respectively, with frequencies of 3252 cm^{-1} (after scaling by 0.9) and 3378 cm^{-1}. Comparison with the experimental values[24] of r_e = 0.971 Å and ν_0 = 3569 cm^{-1} shows that the MP2 results overestimate r_e

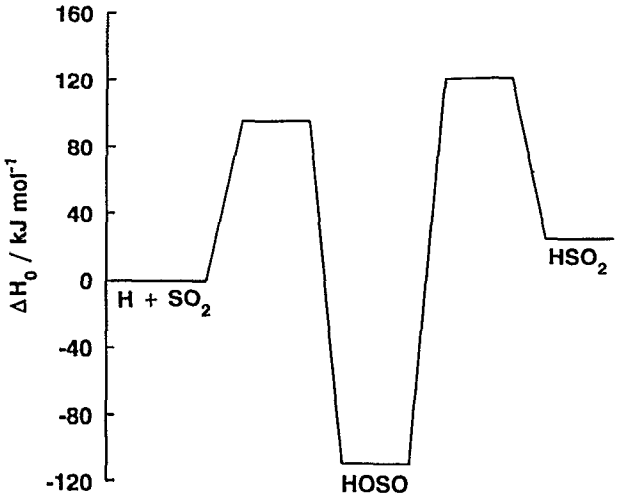

FIG. 2. The potential energy surface for $H + SO_2$ calculated at the PMP4/6-31G*//MP2/3-21G(*) level and incorporating zero-point vibrational energy calculated at the MP2/3-21G(*) level. The ordinate represents enthalpy relative to $H + SO_2$ at 0 K.

by 0.04 Å and underestimate ν_0 by 5%, consistent with the error limits proposed. For SO, the HF/3-21G(*) geometry and scaled frequencies of $r_e = 1.486$ Å and $\nu_0 = 1129\ cm^{-1}$ are within 1% of the experimental values, 1.481 Å and 1136 cm^{-1}.[24] However, MP2 calculations do not describe SO satisfactorily: An apparent minimum lies at $r_e = 1.547$ Å where the HF wave function is unstable, which invalidates energy and frequency calculations made with MP methods.

We may also compare the calculated and experimental thermochemistries for $H + SO_2 \rightarrow OH + SO$. We employ PMP4/6-31G*//MP2/3-21G(*) data (with the exception of SO, for which PMP4/6-31G*//HF/3-21G(*) data are chosen) combined with *ab initio* frequencies to derive the enthalpy change at 0 K, $\Delta H_0 = 108$ kJ mol^{-1}. The experimental value is $\Delta H_0 = 123$ kJ mol^{-1},[24] which suggests we may crudely estimate the uncertainty in *ab initio* energies as at least $\pm$ 15 kJ mol^{-1}. This energy uncertainty translates into an uncertainty in equilibrium or rate constants of a factor of about 3 at 2000 K, increasing to a factor of 400 at room temperature. Thus all *ab initio* equilibrium and rate constants must only be regarded as order of magnitude estimates.

B. HSO_2 adduct

The present HF/3-21G(*) C_s geometry for the $SO_2 \cdot H$ isomer with H bonded to S (see Fig. 1 and Table I) is similar to that derived with a very small STO-3G(*) atomic basis set by Boyd *et al.*[15] [$\theta = 124.7°$, $r(SO) = 1.476$ Å, $r(SH) = 1.362$ Å, $\psi = 105.1°$]. We also optimized the geometry at the HF/6-31G* level: The results in Table I show there is negligible basis set dependence at the HF level. We note that the structure calculated at the HF level by Hinchliffe[14] [$\theta = 132°$, $r(SO) = 1.458$ Å, $r(SH) = 1.336$ Å, $\psi = 105°$] has an inconsistently large OSO angle θ. The data in Table I demonstrate that inclusion of electron correlation at the MP2 level has little influence on the geometry.

Our HF/3-21G(*) calculations also located an asymmetrical C_1 HSO_2 structure, with all real frequencies, and a similar structure was found at the HF/6-31G* level. A TS with a single complex frequency lies between the C_s and C_1 structures. However, attempts to optimize the C_1 structure at the higher MP2 level led only to the symmetrical C_s form, from which we conclude that the C_1 form does not correspond to a real adduct.

Our best estimate of ΔH_0 for the reaction

$$H + SO_2 + Ar \rightarrow HSO_2 + Ar \qquad (3)$$

at the PMP4/6-31G*//MP2/3-21G(*) level (including ZPE), is + 25 kJ mol^{-1} at 0 K (see Table II). This predicted endothermicity can be contrasted to the HF/STO-3G(*) estimate of $\Delta H_0 = -142$ kJ mol^{-1} by Boyd *et al.*[15] A small basis set was employed, and neither ZPE nor electron correlation was included. We therefore believe our result is more reliable. We used our ΔH_0 combined with MP2/3-21G(*) structures and frequencies to calculate the equilibrium constant K_p for reaction (3) by statistical mechanics.[25] At 2000 K, K_p is about 10^{-6} atm^{-1}, and decreases with decreasing temperature to about 10^{-8} atm^{-1} at 298 K. The equilibrium ratio $[HSO_2]:[H]$ when $[H] \ll [SO_2]$ and K_p is small is given by $p(SO_2) \times K_p$, so it is clear that reaction (3) alone cannot be a significant sink for atomic H either in room temperature experiments or in SO_2-seeded flames. We have also estimated the maximum H-atom removal rate possible if HSO_2 can react with H with a rate constant $k_2 = 10^{-10}$ molecule^{-1} cm^3 s^{-1} at 2000 K. The assumption of an initial [H] of 10^{16} cm^{-3}, and a high $[SO_2]$ of 2×10^{18} cm^{-3}, leads to a minimum half-life for second-order removal of H of about 1 s. This is too slow to be significant and we therefore conclude that HSO_2 is insufficiently stable to be important in the chemistry of flames.

HSO_2 was proposed by McDowell *et al.*[13] as the radical species formed by irradiation of an HI/SO_2 mixture in frozen Kr, followed by repeated annealing, and detected by ESR. A very recent study by Fender *et al.*[26] also involved irradiation of mixtures of SO_2 with HI or H_2S, in a solid Ar matrix. However, these workers identified sulfinic acid (HSO_2H) as the sole product on the basis of ir spectroscopy. Presumably, the radical species detected in the earlier matrix-isolation study are formed only in the annealing steps.

C. Transition state for $HSO_2 \rightarrow H + SO_2$

The dissociation of C_s HSO_2 to $H + SO_2$, reaction (-3), was initially investigated at the HF/3-21G(*) level. As the S–H distance is increased, the energy rises, but the HF PES is discontinuous and at $r(SH) \approx 1.9$ Å, there is a switch to a lower energy C_1 geometry. A C_1 TS was located, but in the light of the observation of spurious C_1 HSO_2 (Sec. III B), and because this C_1 TS could not be confirmed at the MP2 level, we believe the TS may also be an artifact. MP2/3-21G(*) calculations located a possible C_s TS with structure $\theta = 119.4°$, $\psi = 105.1°$, $r(SO) = 1.469$ Å, $r(SH) = 1.839$ Å. However, vibrational frequencies could not be obtained because of HF instability.[22] This possible TS has an electronic energy 49 kJ mol^{-1} higher than C_s HSO_2

at the MP2/3–21G(*) level, but changes in ZPE must also be considered. During dissociation, 39 kJ mol^{-1} of ZPE are lost, which means that the energy barrier in the vibrationally adiabatic PES may be small. Even if the barrier were as much as 40 kJ mol^{-1}, a likely rate constant for room temperature high-pressure unimolecular dissociation, on the assumption of a typical preexponential factor of 10^{13} s^{-1},[27] is about 10^6 s^{-1}. Concentrations of the HSO_2 radical above equilibrium will therefore be very short lived in the gas phase.

D. HOSO adduct

We have found a single stable minimum at the HF/3–21G(*) level where the H atom is bonded to an O atom and twisted out of the SO_2 plane (see Table I). HF/6–31G* calculations yield a similar structure and confirm the absence of basis-set dependence. This staggered configuration is similar to that described by Boyd *et al.*[15] The planar *cis* and *trans* HOSO conformers are both saddlepoints at the HF/3–21G(*) level, with energies (including ZPE) of 29 and 6 kJ mol^{-1} above the staggered form. Again, HF/6–31G* calculations are in accord and also show these conformations to be saddlepoints. By contrast, MP2/3–21G(*) calculations indicate that the *cis* structure is a stable minimum, the *trans* structure remains a TS and there is no staggered stationary point. The *cis* form may be stabilized by intramolecular hydrogen bonding. The energy barrier, including changes in ZPE, to rotation of OH about the S–O bond is 19 kJ mol^{-1} at the PMP4/6–31G*//MP2/3–21G(*) level (see Table II). The vibrational frequency of the mode of *cis* HOSO which corresponds to motion of the H atom out of the SO_2 plane is low, about 100 cm^{-1}, which is another indication of easy internal rotation. This torsional frequency, coupled with the reduced moment of inertia for internal rotation of 1.46×10^{-47} kg m^2, corresponds to a rotational barrier of 6 kJ mol^{-1} if a sinusoidal potential is assumed.[28] These two measures are consistent with a small rotational barrier of around 10 kJ mol^{-1}. We have therefore decided to replace the slightly hindered internal rotor with a free rotor for the purposes of thermodynamic calculations, which should be a good approximation at elevated temperatures.

Our best estimate (Table II) of the H–OSO bond energy is $D_0 = 109$ kJ mol^{-1}. By chance, this is close to the D_0 recommended by Atkinson *et al.* for H–SO_2.[16] We have calculated K_c for the reaction

$$H + SO_2 + Ar \rightarrow HOSO + Ar \qquad (4)$$

from 298 to 2000 K, and fit the results to yield $K_c = 1.1\times10^{-23}\exp(1.35\times10^4\ \mathrm{K/T})$ molecule^{-1} cm^3. This implies values of K_p for reaction (4) at 298 and 2000 K of 1.2×10^{16} and 3.9×10^{-2} atm^{-1}, respectively, so that HOSO is sufficiently stable to be an important sink for atomic H in flames.

Three potential unimolecular decomposition pathways for the HOSO adduct are considered in the following sections: (i) dissociation back to H + SO_2, (ii) rearrangement to HSO_2, and (iii) dissociation to OH + SO.

E. Transition state for HOSO → H + SO_2

The transition state for dissociation of HOSO to H + SO_2, the most exothermic possible dissociation products considered, has been characterized at the HF and MP2 levels of calculation. The results (Table I) show that the MP2 calculations yield a tighter TS, with a shorter O–H distance than at the HF level and with higher frequencies. The MP2 results also indicate that the OSO moiety has relaxed to essentially the equilibrium SO_2 geometry. While small barriers to association are typical for recombination of a radical with a closed shell molecule,[29] PMP4/6–31G*//MP2/3–21G(*) calculations indicate a remarkably large energy barrier for reaction (4) of 95 kJ mol^{-1} relative to H + SO_2. This TS shows a strong variation of the O–H distance with the level of calculation, decreasing from 1.785 Å at the HF/3–21G(*) level to 1.550 Å at the MP2/3–21G(*) level. This uncertainty in r(OH) could lead to significant error in the energy of the TS because the PES curves steeply there, as reflected by the complex frequency of the order of $1000i$ cm^{-1}. For example, calculation of the PMP4/6–31G* energy at the HF rather than MP2 geometry lowers the barrier by 36 kJ mol^{-1}. We therefore checked the TS geometry at higher levels of theory to see whether the long or short O–H partial bond is supported. The HF/6–31G* geometry has r(OH) = 1.664 Å (Table I) while the complete MP2/6–31G* geometry is $r(SO_1) = 1.441$ Å, $r(SO_2) = 1.460$ Å, $r(O_2H) = 1.507$ Å, $\theta = 120.2°$, $\phi = 125.2°$, and $\delta = 78.2°$ (see Fig. 1). These results suggest that the MP2/3–21G(*) geometry is indeed reliable.

We have analyzed the kinetics of unimolecular dissociation by means of Rice–Ramsberger–Kassel–Marcus (RRKM) theory, following the procedures described by Gilbert and co-workers.[29,30] The two rotations, of both HOSO and the TS, with the smallest moments of inertia were taken as inactive (whose energy is unavailable for crossing the potential barrier) and in each case the third rotation was taken to be active. The Lennard-Jones collision rate between HOSO and Ar bath gas was estimated by means of the Lennard-Jones parameters for Ar and SO_2,[31] to yield $\sigma_{LJ} = 3.854$ Å and $\epsilon_{LJ} = 177$ K. A weak-collision "exponential down" model for energy transfer between excited HOSO and Ar was assumed.[29] This leads to a calculated collision efficiency β_c of 0.48 at 298 K, decreasing to 0.036 at 2000 K. These values are in line with typical β values at room and flame temperatures.[32] We used the UNIMOL program[30] to calculate falloff curves for reaction (− 4) at 298 and 2000 K, and the results are drawn in Fig. 3. The reaction will be in the third-order region under most flame conditions, but falloff behavior would, in principle, be evident at 298 K at pressures of the order of 100 Torr. As shown below, the reaction will, however, be too slow to measure at room tions, but falloff behavior would, in principle, be evident at 298 K at pressures of the order of 100 Torr. As shown below, the reaction will, however, be too slow to measure at room temperature.

We have also calculated the low-pressure second-order dissociation rate constant k_{-4} as a function of temperature. The dissociation rate will be negligible for $T < 700$ K. Because the dissociation step involves motion of an H atom

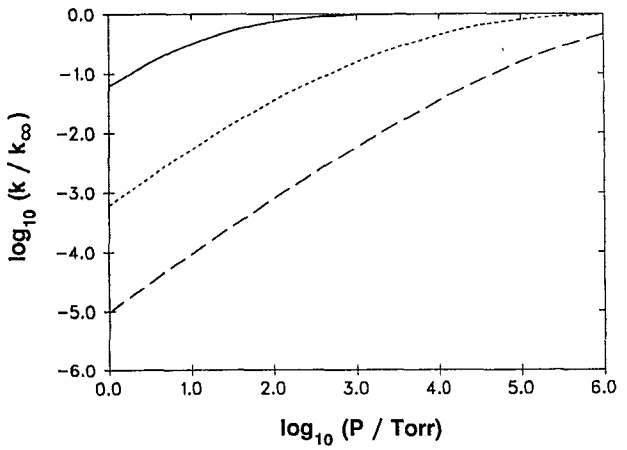

FIG. 3. Falloff curves for $H + SO_2 + Ar \rightleftarrows HOSO + Ar$ at (i) 298 K, solid line; (ii) 1000 K, short dashes; (iii) 2000 K, long dashes.

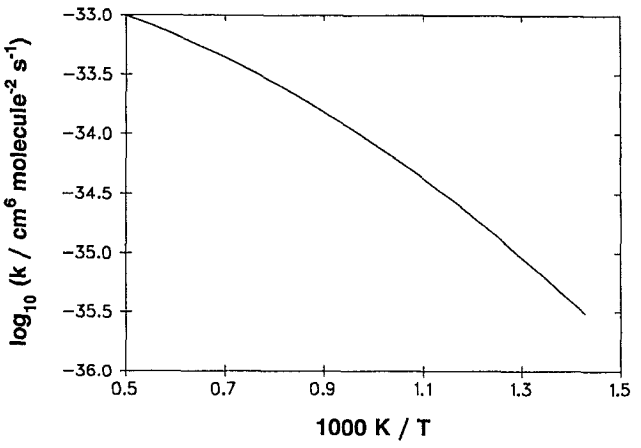

FIG. 5. Arrhenius plot of third-order rate constant k_4 for $H + SO_2 + Ar \rightarrow HOSO + Ar$.

over a potential barrier the possibility of quantum mechanical tunneling exists. We have crudely estimated a tunneling correction factor by fitting an Eckart potential[33] to the vibrationally adiabatic PES, as employed previously to analyze the decomposition of HNNO,[34] to derive the tunneling-corrected rate constant plotted on Fig. 4. The correction factor decreases from 4×10^4 at 298 K, through 2.8 at 700 K to 1.1 at 2000 K. The final results for $T = 700$ to 2000 K can be summarized by $k_{-4} \approx 2.5\times10^{-9}\ \exp(-19\,800\ \mathrm{K/T})$ $\mathrm{cm^3\ molecule^{-1}\ s^{-1}}$.

The equilibrium constant for reaction (4) (see Sec. III D) is used to derive the third-order rate constant for $H + SO_2$ recombination, corrected for tunneling and plotted on Fig. 5. For $T \geqslant 700$ K an approximate expression is $k_4 \approx 3.1\times10^{-32}\ \exp(-6300\ \mathrm{K/T})\ \mathrm{cm^6\ molecule^{-2}\ s^{-1}}$. An interesting feature is that the activation energy for recombination is about 52 kJ $\mathrm{mol^{-1}}$, which is considerably smaller than the energy barrier of 95 kJ $\mathrm{mol^{-1}}$. This reflects two factors: At low temperatures tunneling enhances reactivity, and more importantly, at high temperatures collisional stabilization of nascent excited HOSO is inefficient and reduces k_4. This latter effect also causes the non-Arrhenius curvature of Fig. 5. At 298 K, k_4 is predicted to be negligibly slow ($k_4 \approx 10^{-40}\ \mathrm{cm^6\ molecule^{-2}\ s^{-1}}$). This is consistent with the lack of reaction noted by Fair and Thrush who used a fast-flow technique,[7] and the absence of reaction seen in our own laboratory where flash photolysis/resonance fluorescence experiments were performed.[9] Both studies employed Ar bath gas and suggest $k_4 < 1.5\times10^{-33}\ \mathrm{cm^6\ molecule^{-2}\ s^{-1}}$ at room temperature. Our experiments also give an upper limit to k_4 of $< 1.5\times10^{-33}\ \mathrm{cm^6\ molecule^{-2}\ s^{-1}}$ at 500 K, consistent with a predicted k_4 there of $\approx 10^{-38}\ \mathrm{cm^6\ molecule^{-2}\ s^{-1}}$. The presence of a large energy barrier thus dramatically slows $H + SO_2$ recombination. This reaction can be contrasted to the recombination of valence isoelectronic Na with SO_2, which has little or no barrier and for which the third-order rate constant is about 3×10^{-29} $\mathrm{cm^6\ molecule^{-2}\ s^{-1}}$ at $T \approx 800$ K.[35]

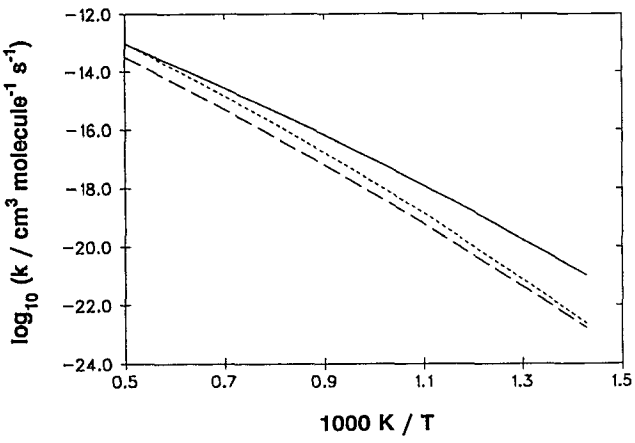

FIG. 4. Arrhenius plot of low-pressure limiting rate constants for HOSO + Ar reacting to (i) $H + SO_2$ (k_{-4}), solid line; (ii) HSO_2 (k_5), long dashes; (iii) OH + SO (k_6), short dashes.

We now compare our results with combustion studies. Flame models do not discriminate between formation of HOSO and HSO_2 and yield $k_1 = k_3 + k_4$. Because of the unfavorable thermochemistry predicted for reaction (3) (see Sec. III B), we assume $k_1 \approx k_4$. For $T \approx 2000$ K Baulch *et al.* recommend $k_4 = 1.4\times10^{-32}\ \mathrm{cm^6\ molecule^{-2}\ s^{-1}}$ with error limits of at least 50%,[36] based on combustion studies. This value of k_4 is about an order of magnitude greater than the *ab initio* result $k_4 \approx 10^{-33}\ \mathrm{cm^6\ molecule^{-2}\ s^{-1}}$ at 2000 K. One reason for this discrepancy is that recombination rate constants are dependent on the bath gas. An example is the reaction $O + SO_2 + M \rightarrow SO_3 + M$, where the rate constant for $M = SO_2$ is about ten times greater than for M = Ar.[37] The presence of efficient quenching species such as SO_2 and H_2O in flames may increase k_4 above the value calculated here for M = Ar. It is also possible that the *ab initio* barrier to reaction (4) may be significantly overestimated, or that the interpretation of the flame results, which rests partly on questionable H–OSO bond energies, may need to be revised.

F. Transition state for HOSO→HSO$_2$

A second possible unimolecular channel for HOSO is isomerization to the HSO_2 structure,

$$HOSO + Ar \rightarrow HSO_2 + Ar. \quad (5)$$

As noted in Sec. III C, HSO_2 will, in turn, rapidly decompose to H + SO_2, so reaction (5) is effectively an alternate pathway to H + SO_2 at flame temperatures. Comparison of structures obtained with the 3–21G(*) and 6–31G* basis sets show there is no significant basis set dependence at the HF level (Table I). The MP2/3–21G(*) transition state parameters summarized in Table I together with the PMP4/6–31G*//MP2/3–21G(*) energy (Table II) were employed to analyze the kinetics for reaction (5) in the same way as outlined in Sec. III E. The energy barrier, relative to HOSO, is 230 kJ mol^{-1} which is similar to that predicted for the isomerization of HSO to HOS.[38] The tunneling-corrected results are plotted on Fig. 4. The predicted k_5 is 4.6×10^{-9} exp(− 23 100 K/T)cm^3 molecule^{-1}s^{-1} over the range 700 to 2000 K. For $T>1000$ K, k_5 is about a third of k_{-4}, because of the greater barrier to isomerization. Thus k_5 is not large enough to change the order of magnitude estimates of the kinetics for H + $SO_2 \rightleftarrows$ HOSO significantly.

G. Transition state for HOSO→OH+SO

A preliminary search of the PES for the process

$$HOSO + Ar \rightarrow OH + SO + Ar \quad (6)$$

at the HF/3–21G(*) level found no evidence of an energy barrier beyond the reaction endothermicity. In order to analyze the kinetics of reaction (6) for $T\geqslant700$ K, we applied canonical variational transition state theory to locate an approximate TS.[29] We considered the OS–OH bond to correspond to the reaction coordinate r, and assumed free rotation about this bond for all values of r (see Sec. III D). A crude force constant for small displacements along the reaction coordinate was obtained by slightly varying r from the optimized value in HOSO at the MP2 level, and recalculating the MP2 energy while all other geometry parameters were held constant. A Morse potential was then fit as a function of r, with parameters $D_e = 123$ kJ mol^{-1} and $\beta = 3.05$ Å^{-1}. The O–H and S–O vibrational frequencies in the TS were taken to be equal to those for SO and OH (Sec. III A). Rotational constants for the rocking motions of the SO and OH fragments in the TS were estimated as 16.8 and 0.48 cm^{-1}.[30] Trial and error was employed to find the value of r, about 3.5 Å, which minimized the high-pressure unimolecular decomposition rate constant at each T. Calculations at $T = 1400$ K show that for P < 1000 Torr, k_6 is within 10% or less of the low-pressure limit, consistent with falloff curves for k_{-4} (Fig. 3). The temperature dependence of k_6 is plotted on Fig. 4, and can be summarized as $k_6 = 2.3\times10^{-8}$ exp(− 23 900 K/T) cm^3 molecule^{-1} s^{-1} for $T\geqslant700$ K. From 1000 to 2000 K, k_6 varies from about 0.1 to 1 times k_{-4}, and this channel may need to be considered in combustion models.

The absence of any barrier to reaction (6) suggests that a possible pathway for the recombination reaction of OH with SO is via initial formation of HOSO. This recombination rate constant has been measured at room temperature to be about 9×10^{-11} cm^3 molecule^{-1} s^{-1},[39] which is close to gas kinetic and therefore consistent with the absence of a barrier. Products have yet to be determined experimentally; The assumed products of H + SO_2 might be formed directly or by fragmentation of excited HOSO as part of a chemical activation mechanism.

IV. CONCLUSIONS

Two adducts can be formed by recombination of H with SO_2. HOSO is predicted to be the more stable, with an HOSO bond energy of 190 kJ mol^{-1}, whereas HSO_2 is endothermic by 25 kJ mol^{-1} with respect to H + SO_2. Vibrational frequencies of the adducts have been calculated, which should aid in their identification by infrared spectroscopy. Several conformers of HOSO were examined: Inclusion of electron correlation suggests that only planar *cis* HOSO is a stable species. Investigation of the transition state between HOSO and H + SO_2 suggests the presence of a large barrier, which is consistent with the lack of reaction noted experimentally at $T\leqslant500$ K. The H + SO_2 + Ar recombination rate constant is estimated to be about 10^{-33} cm^6 molecule^{-2} s^{-1} at 2000 K, about an order of magnitude smaller than estimated from combustion studies. These studies may need revision in the light of the new thermochemistry calculated here, or else the barrier to recombination may be smaller than predicted. Two other unimolecular channels for HOSO, isomerization to HSO_2 and decomposition to SO + OH, have also been characterized. The results suggest that a possible reaction mechanism for the reaction of OH with SO may be via an excited HOSO intermediate.

ACKNOWLEDGMENTS

We are grateful for support from the R. A. Welch Foundation (Grant No. B-1174) and from UNT Organized Research Funds. Computer time was provided by UNT and the NSF Pittsburgh Supercomputing Center, through Grant No. CHE900059P.

[1]M. R. Zacharia and O. I. Smith, Combust. Flame **69**, 125 (1987).
[2]A. S. Kallend, Trans. Faraday Soc. **63**, 2442 (1967).
[3]C. J. Halstead and D. R. Jenkins, Trans. Faraday Soc. **65**, 3013 (1969).
[4]R. A. Drurie, G. M. Johnson, and M. Y. Smith, Combust. Flame **17**, 197 (1971).
[5]C. F. Cullis and M. F. R. Mulcahy, Combust. Flame **18**, 225 (1972).
[6]A. S. Kallend, Combust. Flame **19**, 227 (1972).
[7]R. W. Fair and B. A. Thrush, Trans. Faraday Soc. **65**, 1550 (1969).
[8]K. Schofield, J. Phys. Chem. Ref. Data **2**, 25 (1973).
[9]Y. Shi, L. Ding, and P. Marshall (unpublished work). H atoms were generated by flash photolysis of NH_3 in the presence of excess SO_2 in an Ar bath gas, and monitored by time-resolved atomic resonance fluorescence.
[10]E. B. Gordon, B. I. Ivanov, A. P. Perminov, and V. E. Balalaev, Chem. Phys. **35**, 79 (1978).
[11]V. A. Arutyunov, V. I. Vedeneev, V. A. Ushakov, and V. V. Shumova, Kinet. Catal. **31**, 6 (1990).
[12]E. R. Lovejoy, N. S. Wang, and C. J. Howard, J. Phys. Chem. **91**, 5749 (1987).
[13]C. A. McDowell, F. G. Herring, and J. C. Tait, J. Chem. Phys. **63**, 3278 (1975).
[14]A. Hinchliffe, J. Mol. Struct. **71**, 349 (1981).
[15]R. J. Boyd, A. Gupta, R. F. Langler, S. P. Lownie, and J. A. Pincock, Can. J. Chem. **58**, 331 (1980).
[16]R. Atkinson, D. L. Baulch, R. A. Cox, R. F. Hampson, Jr., J. A. Kerr, and

J. Troe, J. Phys. Chem. Ref. Data **18**, 881 (1989).
[17]W. J. Hehre, L. Radom, P. v. R. Schleyer, and J. A. Pople, *Ab Initio Molecular Orbital Theory* (Wiley, New York, 1986).
[18]M. J. Frisch, M. Head-Gordon, H. B. Schlegel, K. Raghavachari, J. S. Binkley, C. Gonzalez, D. J. Defrees, D. J. Fox, R. A. Whiteside, R. Seeger, C. F. Melius, J. Baker, R. L. Martin, L. R. Kahn, J. J. P. Stewart, E. M. Fluder, S. Topiol, and J. A. Pople, GAUSSIAN 88 (Gaussian, Pittsburgh, 1988).
[19]M. J. Frisch, M. Head-Gordon, G. W. Trucks, J. B. Foresman, H. B. Schlegel, K. Raghavachari, M. A. Robb, J. S. Binkley, C. Gonzalez, D. J. Defrees, D. J. Fox, R. A. Whiteside, R. Seeger, C. F. Melius, J. Baker, R. L. Martin, L. R. Kahn, J. J. P. Stewart, S. Topiol, and J. A. Pople, GAUSSIAN 90 (Gaussian, Pittsburgh, 1990).
[20]W. J. Pietro, M. M. Francl, W. J. Hehre, D. J. deFrees, J. A. Pople, and J. S. Binkley, J. Am. Chem. Soc. **104**, 5039 (1982).
[21]M. M. Francl, W. J. Pietro, W. J. Hehre, J. S. Binkley, M. S. Gordon, D. J. DeFrees, and J. A. Pople, J. Chem. Phys. **77**, 3654 (1982).
[22]R. Seeger and J. A. Pople, J. Chem. Phys. **66**, 3045 (1977).
[23]H. B. Schlegel, J. Chem. Phys. **84**, 4530 (1986).
[24]M. W. Chase, Jr., C. A. Davies, J. R. Downey, Jr., D. J. Frurip, R. A. McDonald, and A. N. Syverud, JANAF Thermochemical Tables, 3rd ed. [J. Phys. Chem. Ref. Data **14**, Suppl. No. 1 (1985)].
[25]G. N. Lewis and M. Randall, *Thermodynamics*, 2nd ed., revised by K. S. Pitzer and L. Brewer (McGraw-Hill, New York, 1961) Ch. 27.
[26]M. A. Fender, Y. M. Sayed, and F. T. Prochaska, J. Phys. Chem. **95**, 2811 (1991).
[27]S. W. Benson, *Thermochemical Kinetics* (Wiley-Interscience, New York, 1976), ch. 3.
[28]K. S. Pitzer and W. D. Gwinn, J. Chem. Phys. **10**, 428 (1942).
[29]R. G. Gilbert and S. C. Smith, *Theory of Unimolecular and Recombination Reactions* (Blackwell, Oxford, 1990).
[30]R. G. Gilbert, M. J. T. Jordan, and S. C. Smith, UNIMOL program, 1990 (see Ref. 29).
[31]R. C. Reid and T. K. Sherwood, *The Properties of Gases and Liquids* (McGraw-Hill, New York, 1958).
[32]W. C. Gardiner, Jr., and J. Troe, in *Combusion Chemistry*, edited by W. C. Gardiner, Jr. (Springer-Verlag, New York, 1984), Ch. 4.
[33]H. S. Johnston, *Gas Phase Reaction Rate Theory* (Ronald, New York, 1966), Ch. 2.
[34]P. Marshall, A. Fontijn, and C. F. Melius, J. Chem. Phys. **86**, 5540 (1987).
[35]Y. Shi and P. Marshall, J. Phys. Chem. **95**, 1654 (1991).
[36]D. L. Baulch, D. D. Drysdale, J. Duxbury, and S. J. Grant, *Evaluated Kinetic Data for High Temperature Reactions*, Vol. 3 (Butterworths, London, 1976).
[37]D. L. Singleton and R. J. Cvetanovic, J. Phys. Chem. Ref. Data **17**, 1377 (1988).
[38]P. L. M. Plummer, J. Chem. Phys. **92**, 6627 (1990).
[39]W. B. DeMore, M. J. Molina, S. P. Sander, D. M. Golden, R. F. Hampson, M. J. Kurylo, C. J. Howard, and A. R. Ravishankara, *Chemical Kinetics and Photochemical Data for Use in Stratospheric Modeling. Evaluation No. 8* (Jet Propulsion Laboratory, Pasadena, 1987).